Beta-alpha angular correlations in mass 8

R. D. McKeown, G. T. Garvey, and C. A. Gagliardi
Argonne National Laboratory, Argonne, Illinois 60439
(Received 12 February 1980)

A detailed study of the $\beta^{\mp}$-α angular correlations in the ^{8}Li(β^-) and ^{8}B(β^+) decays was performed. Since these decays proceed to the 2α continuum, detection of both alpha particles enabled determination of various correlations as functions of the final-state energy. The experimental results show a small ($\approx$ 15% of weak magnetism) deviation from the conserved vector current prediction which is dependent on the final-state energy. An effect of this size cannot be interpreted as convincing evidence for the presence of second-class currents or a breakdown of conserved vector current theory. However, the inclusion of the vector second-forbidden terms in the nuclear weak current as predicted by the conserved vector current theory is crucial to obtain even approximate agreement with the experimental results.

[RADIOACTIVITY ^{8}Li, ^{8}B; measured $\beta\alpha$ angular correlation, final-state energy dependence. Model independent test of CVC and second-class currents.]

I. INTRODUCTION

Angular correlation measurements in nuclear beta decay can serve as useful probes of fundamental symmetries of the weak hadronic current.[1] In particular, the conserved vector current (CVC) hypothesis[2] and the existence of second-class currents[3] (SCC) can be tested by such experiments. Since the presence of second-class terms would introduce serious theoretical difficulties in renormalizable gauge theories,[4] much effort has been expended in recent years to study this question via nuclear beta decay experiments. Due to the small momentum transfer, the measured quantities in these experiments are small (of order E/M_n, where E is the β energy and M_n the nucleon mass) and, therefore, the experiments are difficult and often quite sensitive to systematic errors. Although previous measurements in the $A=8$ system have not shown any effect attributable to SCC, several experimental results in other nuclear systems seemed to require the presence of large second-class terms.[5]

As can be seen in Fig. 1, the $\beta^{\mp}$ decays in the $A=8$ system proceed to a broad final-state distribution in the 2α continuum dominated by the first excited state in ^{8}Be. A comparison of the β-α angular correlations in the β^- and β^+ decays coupled with knowledge of the isovector radiative widths of the analog gamma decay (via application of CVC) is sensitive to the presence of SCC. Recent investigations of the analog γ decay[6,7] indicated two features which motivated more detailed measurements of the β-α angular correlations. First, the final-state distribution populated by the γ decay is somewhat different than that populated in β decay (with phase space removed), implying a final-state energy dependence to the β-α angular correlation (assuming CVC). Second, the analog γ decay has an unusually large isovector $E2/M1$ mixing ratio, so that the β-α angular correlation is sensitive to the term in the weak vector current corresponding to the electric quadrupole term in the electromagnetic current. At present, this is the only set of measurements which tests the application of CVC to this term in the vector current.

Previous measurements of the β-α angular correlations in the $A=8$ system[8] measured the integrated effects for the entire final-state distribution. Although the analysis of these results did not indicate the presence of SCC, these experi-

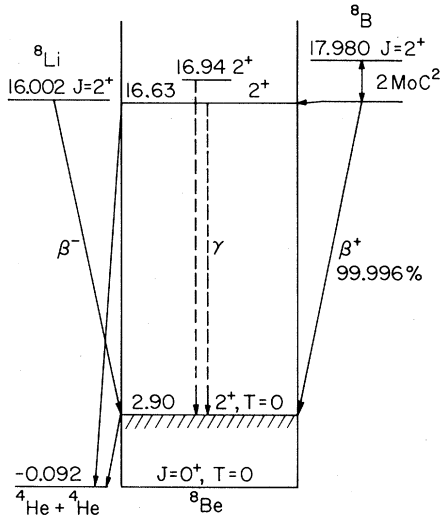

FIG. 1. $A=8$ energy level diagram showing the relevant nuclear structure for β-α angular correlation and analog γ-decay experiments. The analog of the ^{8}Li and ^{8}B ground states is mixed with a $T=0$ state to form the 16.63–16.94 doublet.

ments did not produce expected theoretical results for the $\cos(\theta)$ term in the angular correlation which is predominantly kinematic in origin. The goal of the present work was to measure the final-state energy dependence of the $\beta^{\mp}$-α angular correlations in mass 8 and to attempt to clarify some of these other issues.

II. THEORETICAL ANALYSIS

Correlation experiments in beta decay can be analyzed in a model independent fashion by using the elementary particle approach. This method has been reviewed by Holstein,[1] and we utilize the notation of that work in the following. The nuclear states are considered as objects with spin, parity, and mass with all internal structure effects contained in various form factors associated with the nuclear weak current.

The form of the $\beta^{\mp}$-α angular correlation can be obtained from the expressions given by Holstein to be

$$N_{\mp}(\theta,E,E_0)=F(E,E_0)[1+a_{\mp}(E,E_0)\cos\theta + p_{\mp}(E,E_0)\cos^2\theta], \quad (1)$$

where E = beta energy, E_0 = end-point energy, and θ is the angle between the $\beta^{\mp}$ and α momenta (we have set v/c for the $e^{\mp}$ to 1 in this expression). The functions $a(E,E_0)$ and $p(E,E_0)$ are given by (for a $2^+ \to 2^+$ Gamow-Teller decay)

$$a_{\mp}(E,E_0) = -\frac{2E}{Mv^*} + \text{terms higher order in } E/M, \quad (2)$$

$$p_{\mp}(E,E_0)=\frac{E}{2Mc}\left((c-d\pm b)+\frac{1}{(14)^{1/2}}\left\{\left[\pm 3f\pm(\tfrac{3}{2})^{1/2}g\frac{E_0-E}{M}+3j_2\frac{E_0-2E}{2M}\right]\right\}-3/(35)^{1/2}j_3E/M\right), \quad (3)$$

in which M is the nuclear mass, v^* is the velocity of the α particle in the rest frame of the daughter nucleus, and the form factors are defined as follows:

c = Gamow-Teller,

b = weak magnetism,

d = induced tensor,

f,g = second-forbidden form factors in the vector current,

j_2,j_3 = second-forbidden form factors in the axial vector current.

Application of CVC relates b to the isovector $M1$ radiative width of the analog γ decay ($\Gamma_{M1}^{T=1}$) and the form factors f,g to the isovector $E2$ amplitude:

$$b=M\left(\frac{6}{\alpha}\frac{\Gamma_{M1}^{T=1}}{E_\gamma^{\,3}}\right)^{1/2},$$

$$\frac{f}{b}=\left(\frac{3}{10}\right)^{1/2}\delta_1=\pm\frac{3}{10}\left(\frac{\Gamma_{E2}^{T=1}}{\Gamma_{M1}^{T=1}}\right)^{1/2},$$

$$g=-\left(\frac{2}{3}\right)^{1/2}\left(\frac{2M}{E_0}\right)f.$$

Thus, assuming CVC, we can express the difference

$$\delta^- = p_- - p_+ = \frac{E}{m_n}\left\{\frac{b}{Ac}\left[1-\left(\frac{5}{21}\right)^{1/2}\left(1+2\frac{E}{E_0}\right)\delta_1\right]-\frac{d_{11}^{\text{eff}}}{Ac}\right\}, \quad (4)$$

where d_{11}^{eff} represents the contribution of SCC to the various axial vector form factors and A is the nuclear mass number. Small electromagnetic corrections to this expression will be discussed in Sec. VI.

Assuming CVC, the form factors b, c, f, and g have all been measured in other experiments. In this work we shall consider all the form factors contributing to δ^- (and δ^- itself) to be functions of E_x, the final-state excitation energy in ^{8}Be. The E_x dependence of Γ_{M1} is known from γ-decay measurements,[6] while the energy-dependent ft-value data of Wilkinson *et al.*[9] give $c(E_x)$. The excitation energy dependence of δ_1 has not been measured to date, and for the present discussion we will assume δ_1 is linear in E_γ unless explicitly stated otherwise. (This is as one would expect if the $E2$ and $M1$ nuclear matrix elements had the same E_x dependence.)

Measurement of the excitation energy dependence of the β-α angular correlation requires determination of the energies of both α particles in the final state. The sum of E_{α_1} and E_{α_2} is related to the excitation energy in ^{8}Be. In addition, one can form the difference $\Delta E_\alpha = E_{\alpha_1} - E_{\alpha_2}$ to obtain information about the ^{8}Be recoil spectrum, and hence, the momentum distribution of neutrino emission (β-ν-α correlation). At $\theta = 90°$ (α direction perpendicular to β emission) one expects $\Delta E_\alpha \cong 0$ by symmetry. However, for $\theta = 0°$ or $180°$, ΔE_α is nonzero and contains the recoil information. The expression for the spectrum of α particles in coincidence with β particles at $|\hat{n}_1\cdot\hat{p}| = 1$ ($\vec{p}$ = beta momentum, $\hat{n}_1$ = alpha direction) can be shown to be

$$N(\Delta E_\alpha)=\text{const}\left[1-\frac{E}{E_0}\rho-\Delta E_\alpha\frac{\hat{n}_1\cdot\vec{p}}{v_1(E-E_0)}\rho\right] \quad (5)$$

in which v_1 is the velocity of the α emitted in the $\hat{n}_1$ direction (in the laboratory frame) and $\rho = (a^2 - c^2)/(a^2 + c^2)$ with $a(c)$ = Fermi (Gamow-Teller) form factor. Only allowed terms were included in the derivation of Eq. (5).

Since the energy resolution in our measurement of the ΔE_α is not sufficient to analyze the spectrum shape for ρ, it is useful to calculate $\langle \Delta E_\alpha \rangle$, the centroid of this distribution, as a function of ρ, E, and E^0. Then result is (again for $|\hat{n}_1 \cdot \hat{p}| = 1$)

$$\langle \Delta E_\alpha \rangle = -\hat{n}_1 \cdot \hat{p}[(1 - \rho/3)E + (\rho/3)E_0]v^* . \quad (6)$$

III. EXPERIMENTAL TECHNIQUE

The experimental apparatus, shown in Fig. 2, consisted of two interconnected cylinders: a bombardment chamber and a detection chamber. The source activity was produced in the bombardment chamber using a particle beam from the Argonne 4MV Dynamitron, and transported into the detection chamber by a flipper arm for counting. The flipper arm was symmetric under 180° rotation so that a fresh source could be created while counting was taking place. Transit times for 180° rotation were ~0.25 sec with a positioning accuracy of <0.4 mm.

The source of ^{8}Li was produced via the ^{7}Li(d,p) ^{8}Li reaction using a 0.8 MeV deuteron beam incident on natural LiF(30 μg/cm^2) targets with Ni(90 μg/cm^2) backings. The source spot size was 3 mm in diameter. ^{8}B was produced using the ^{6}Li$(^3$He$,n)^8$B reaction by a 3.6 MeV ^{3}He beam. The high energy of the center-of-mass motion and small yield of this reaction causes some difficulty in preparing a high intensity source of ^{8}B in a thin foil. A variation of the technique used by Tribble *et al.*[8] was employed, in which the recoiling ^{8}B nuclei were stopped in a separate thin catcher foil after being degraded in the target foil. The catcher foil alone was then transported into the detection chamber. A sufficiently high rate of production of ^{8}B required a rather intense (~8 μA) ^{3}He beam. Heating of the target and catcher foils presented a severe problem above 1 μA beam current, so a high speed target rotation system (shown in Fig. 3) was employed. The target foils were laid over slots milled in the Al target wheel on a 10 cm diameter circle, and the wheel was rotated at 1500 RPM. These target foils consisted of 200 μg/cm^2 ^{6}LiF on 300 μg/cm^2 copper backings, the copper acting as a degrader foil for recoiling ^{8}B nuclei and as a heat transfer medium. Molybdenum foils (225 μg/cm^2 thick) were used as catcher foils because of the very high melting point (2900 °K) of molybdenum, and the source spot size was limited to 4.5 mm diameter by collimation.

Alpha particles were counted in ORTEC silicon surface barrier detectors which were removed from their standard metal casings and remounted in Lucite frames to reduce scattering of beta particles. The silicon detectors were hung from the top plate of the detection chamber by aluminum tubes. The beta detectors were 7.62 × 7.62 cm pilot B plastic scintillators mounted on tapered light pipes which were coupled to RCA 8575 photomultiplier tubes.

The detector geometry is shown in Fig. 4. The plastic scintillators were collimated to 250 msr solid angles by 1.1 cm thick lead shields. The alpha counters were arranged in pairs, each pair consisting of a small (45 msr solid angle) primary detector and a larger (~1 sr solid angle) secondary detector. The primary counter defined the α direction by acting as a trigger for each event. The large secondary detector then detected, with unit probability, the other α particle corresponding to the same event. Owing to the recoil momentum of the daughter ^{8}Be, the two alpha particles do not emerge at 180° from each other in the laboratory frame, and the secondary α counter

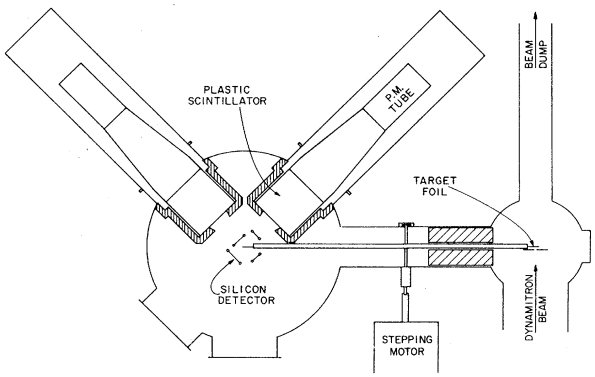

FIG. 2. Schematic diagram of the experimental apparatus.

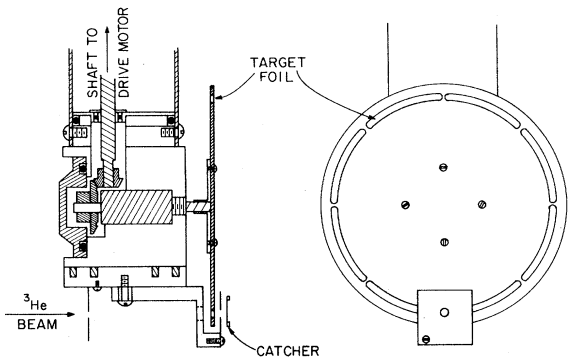

FIG. 3. Target rotation apparatus for production of ^{8}B sources.

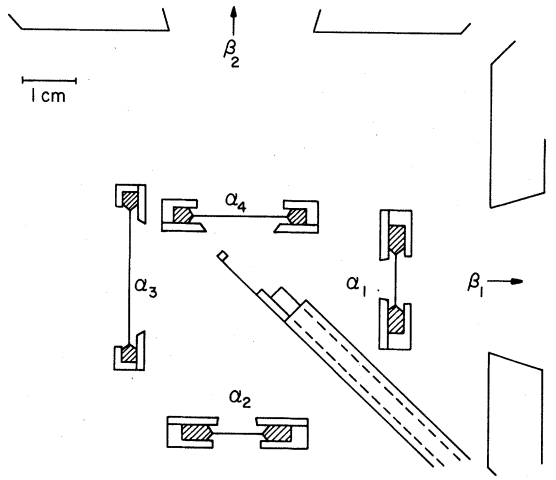

FIG. 4. Detector geometry detail. Detectors α_1 and α_2 are primary counters (50 μm thick). The secondary α detectors are α_3 (100 μm depth—partially depleted) and α_4 (50 μm thick).

must be large enough to ensure counting the second α particle.

A schematic diagram of the electronics is shown in Fig. 5. Linear (energy) and fast timing signals were obtained from each of the six detectors. The timing signals generated time to amplitude converter (TAC) pulses and logic gates to identify the events. The primary α counter thresholds were verified to fire with >99% efficiency for $E_\alpha \geq 180$ keV.

The fast signals from silicon detectors α_1 and α_2 started TAC's 1 and 2, respectively. Both TAC's could be stopped by signals from either beta detector. Alpha singles events were recorded by strobing the analog-to-digital converters (ADC's) with signals obtained by prescaling the "true start" outputs from the TAC's by a factor of 10. These events provided the relative normalization of the α spectra in the data analysis.

Long-term gain drifts in the photomultiplier tubes were a severe problem, as 10–20% variations were noted in the initial runs. Therefore, a light emitting diode (LED) system was installed to facilitate gain stabilization by analog gain control amplifiers. The gain adjustment response time was ~0.1 sec and gain stability was better than 1%. The LED peak in the energy spectrum also served as a check on the accidental coincidence subtraction.

For each event, all eight signals (6 energy and 2 TAC) were digitized and read into a PDP 11/45

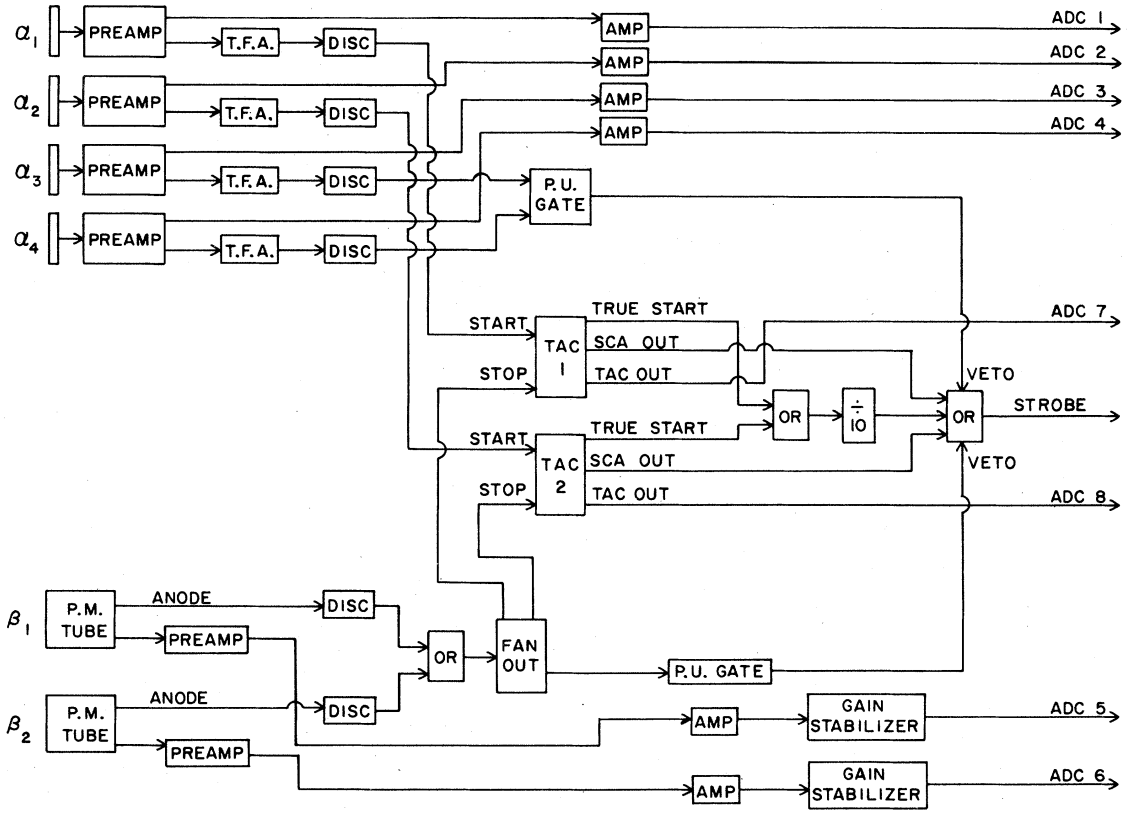

FIG. 5. Schematic diagram of electronics setup.

computer. Singles events were identified as lacking a TAC signal and stored as on-line spectra. In addition to the collection of on-line coincident spectra, the coincidence events were written on magnetic tape in event mode format.

The experiment was run on a 2.4 sec timing cycle, with 2 sec for counting and 0.4 sec for flipper arm rotation, during which data acquisition was inhibited and the dynamitron beam was deflected by electrostatic plates.

IV. DATA ANALYSIS

A. Alpha singles spectra

Singles spectra of the primary α counters (α_1 and α_2) were collected on line to monitor the discriminator thresholds on these detectors. In addition, two-dimensional spectra of the sum of the two α particle energies $\sum E_\alpha$, and their difference ΔE_α, were collected for each of the two α pairs α_{13} and α_{24}. These arrays were especially useful in monitoring the source foil condition by observing the number of single alpha particle (SAP) events, where the secondary α counters did not fire. These were easily identified as a small peak in this spectrum at $\Delta E_\alpha = \sum E_\alpha$. Particularly in the ^{8}Li runs, if the target foil developed a tear, the relative number of SAP events would increase, indicating a foil needed to be changed. A contour plot of this type of spectrum is shown in Fig. 6. These two-dimensional singles spectra were summed in the ΔE_α direction to give one-dimensional singles spectra for relative normalization of the coincident spectra.

The $\sum E_\alpha$ were corrected for energy loss in the target using recent stopping power tables.[10] The excitation energy in ^{8}Be, E_x, was then obtained by subtracting the ground state energy 92 keV.

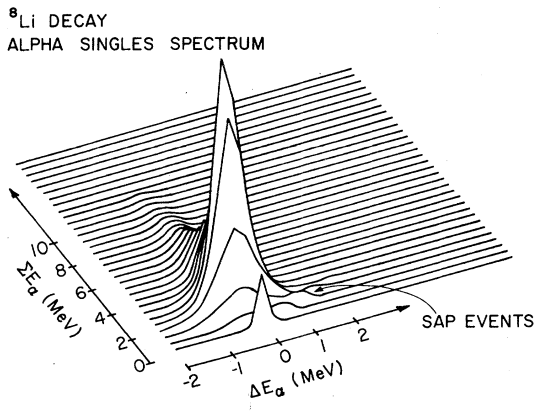

FIG. 6. Perspective plot of alpha singles events for ^{8}Li run. $\sum E_\alpha = E_{\alpha_1} + E_{\alpha_3}$, $\Delta E_\alpha = E_{\alpha_1} - E_{\alpha_3}$, and SAP events are those where detector α_3 did not fire.

B. Coincidence spectra

The coincidence spectra were constructed by setting windows on the TAC signals. "True" and "accidental" windows were set, and the resulting coincidence spectra were subtracted to eliminate contributions from accidental coincidences. The LED peaks in the β spectra indicated the accidental subtraction was accurate to better than 1%. The true to accidental ratio was 37:1 for ^{8}B and 29:1 for ^{8}Li, with most of the accidental events due to neutron detection in the beta counters.

The four coincidence arrays for the analysis of the β-α angular correlation were $N(0)_1$, $N(90)_1$, $N(90)_2$, and $N(180)_2$. The subscripts 1 and 2 refer to beta detectors, and 0, 90, and 180 correspond to $\theta_{\beta\alpha}$ in degrees. These arrays were 32×32 channels of $\sum E_\alpha$ vs E, the beta energy, and were relatively normalized by dividing by the 32-channel α singles spectra described above. This procedure removes experimental asymmetries between the alpha counters associated with solid angle differences, electronics, and ADC nonlinearities. After calibration of the beta detectors (described in the next section), arrays of E_1 and E_2, the energies of the beta channels for detectors 1 and 2, were constructed. Except for small corrections, the β-α angular correlations may be calculated as follows:

$$\Delta_1 = \left[\frac{N(0)_1}{N(90)_1} - 1\right] \Big/ E_1 , \tag{7a}$$

$$\Delta_2 = \left[\frac{N(180)_2}{N(90)_2} - 1\right] \Big/ E_2 , \tag{7b}$$

$$a/E = \frac{\Delta_1 - \Delta_2}{2} , \tag{7c}$$

$$p/E = \frac{\Delta_1 + \Delta_2}{2} , \tag{7d}$$

where a and p refer to the correlation coefficients defined in Eqs. (1)–(3). These equations were modified slightly to include the effects of finite solid angles.

To facilitate comparison with previous experimental results, the data were also analyzed for the $\beta^\pm$-α angular correlations without regard to final-state energy. In order to eliminate events triggered by beta particles (in the primary alpha counters) or noise, the following cuts were made:

(a) The primary α counter was required to have at least 200 keV of energy deposited, and
(b) $\sum E_\alpha > 500$ keV.

The arrays $N(0)_1$, $N(90)_1$, $N(90)_2$, and $N(180)_2$ were then summed in the $\sum E_\alpha$ direction to give one-dimensional arrays and combined as in Eq. (7).

C. Beta spectrum analysis

The response of the plastic scintillators to electrons and positrons affects the measurement of the β-α angular correlations in three important ways: (a) the correlations are beta-energy dependent, so the energy calibration of each detector must be determined; (b) the finite energy resolution of plastic scintillator distorts the measured correlations slightly; and (c) asymmetries between the two beta detectors must be properly handled.

In determining the energy calibration of the beta detectors, an empirical approach was used. The recoil order $[O(E/m_n)]$ effects on the $\theta_{\beta\alpha} = 90°$ beta spectra are quite small, so they can be considered as essentially allowed shapes. The array $N(90)$ is then a set of allowed beta spectra with varying end-point energies determined from the α particle energies. One then generates an ideal allowed spectrum for an end-point energy, convolutes it with a response function, and compares with the corresponding measured spectrum (same end-point energy). The energy calibration and response function are adjusted to reproduce the experimental spectrum for $E > E_0/2$. This process is repeated for different end-point energies to sample different energy regions.

It was found that the experimental spectra could be well reproduced in the region $E_0/3 < E < E_0$ for $6 < E_0 < 16$ MeV with an energy calibration linear in the channel number and a Gaussian response function with the width proportional to the square root of the energy. This is the response one expects from scintillation photon counting statistics alone. Examples of the results are shown in Figs. 7 and 8, where the solid lines are the ideal allowed spectrum shapes and the dashed lines are the convoluted shapes. The sensitivity of the resulting fitted spectra to the energy calibration indicates the calibration is accurate to $\lesssim 1\%$. The excess events at lower energies are mostly due to coincident betas entering the lead collimator and emitting bremsstrahlung photons which then deposit energy in the scintillator via Compton scattering. This was verified by collecting a pulse height spectrum with the β detector collimator hole plugged with lead to prevent beta particles from entering the scintillator. These lower energy regions were ignored in the final data analysis as described in Sec. VI.

To determine the effects of asymmetries in the beta detectors and finite energy resolution, the arrays $N(0)_1$, $N(90)_1$, $N(90)_2$, and $N(180)_2$ were simulated with the empirical resolution and calibration parameters and combined in the same fashion as the actual data [see Eqs. (7a)–(7d)].

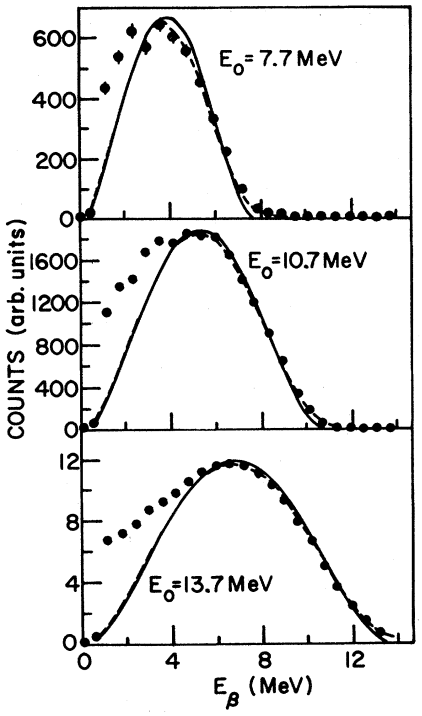

FIG. 7. Sample of ^{8}Li beta spectra for $\theta_{\beta\alpha} = 90°$ at various end points determined by the alpha particle energies. The solid line is an ideal allowed shape and the dashed line is the ideal spectrum convoluted with a gaussian response function.

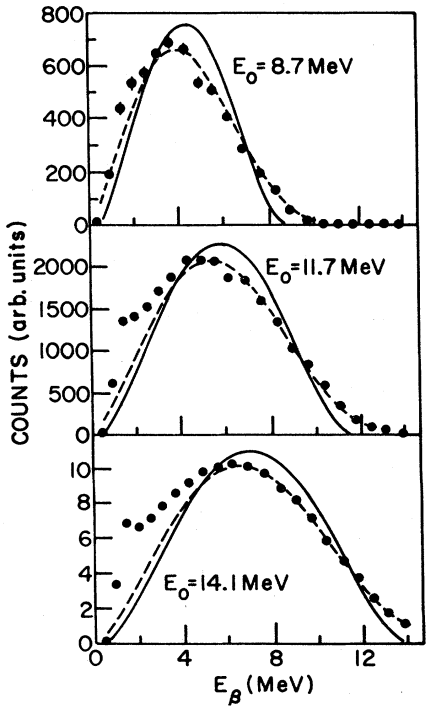

FIG. 8. Same as Fig. 7 for ^{8}B decay.

The calculated effects on the β-α correlations were essentially quadratic in β energy and amounted to at most a 15% correction in any given β-energy bin. Examples of the results of this type of calculation are shown in Fig. 9. The experimental data were corrected for these effects by multiplying by the ratio of ideal to calculated curves obtained from this calculation.

D. Angular correlations in the quantity ΣE_α

A possible problem associated with the measurement of the ^{8}Be excitation energy dependence of the β-α angular correlation is that the value of $\sum E_\alpha$ may be correlated with $\theta_{\beta\alpha}$. At very low excitation energies where the energy loss in the source foil is a large fraction of the total energy, one expects a simulated $\cos(\theta_{\beta\alpha})$ term from the different average trajectories of the secondary α particle associated with different $\theta_{\beta\alpha}$. Above $E_x = 1.5$ MeV the estimated effect is less than 5% of the $\cos(\theta_{\beta\alpha})$ coefficient a/E. Since the effect decreases with increasing E_x, the experimental data were not corrected for this effect.

The single alpha particle (SAP) events are events which contain the wrong information for $\sum E_\alpha$. However, these events (which amount to <1% of all events) were not correlated with $\theta_{\beta\alpha}$ at a statistically significant level and were probably due to large angle multiple scattering of α particles in the source foil. The β-α angular correlation results were insensitive to inclusion or exclusion of these events.

A correction was made to the experimental data to account for the fact that beta particles deposit energy in the silicon counters at certain coincidence angles. All beta particles entering beta detector 2 pass through a counter 4. Therefore, the spectrum $N(180)_2$ was shifted down 20 keV (the energy loss of a beta particle in 50 μm of silicon) in $\sum E_\alpha$ before analysis. Similarly, since ~25% of the β particles entering beta counter 1 pass through α detector 1, the spectrum $N(0)_1$ was shift shifted down 5 keV in $\sum E_\alpha$. A real (not experimentally induced) correlation between $\sum E_\alpha$ and $\theta_{\beta\alpha}$ is also present. This arises because the actual expression for $\sum E_\alpha$ is

$$\sum E_\alpha = 0.092 \text{ MeV} + E_x + E_R \,, \tag{8}$$

where E_R = recoil energy of ^{8}Be* in the laboratory frame. One may calculate E_R as a function of $\theta_{\beta\alpha}$ by averaging over the neutrino direction, and the result is that E_R varies by ~2 keV with a $\cos^2(\theta_{\beta\alpha})$ dependence. Therefore, the excitation energy dependence of the $\cos^2(\theta_{\beta\alpha})$ term in the β-α angular correlation is affected by this mechanism at the 10% level. However, this effect should cancel in the calculation of δ^-, since it contributes equally in the ^{8}B and ^{8}Li decays and varies slowly with excitation energy. However, it does mean that the experimental results for p_-/E and p_+/E are not necessarily correct at individual excitation energies, and this is particularly true of their *sum*. Finally, it should be emphasized that none of the effects described in this section contribute to the experimental results when analyzed without regard for final-state energy.

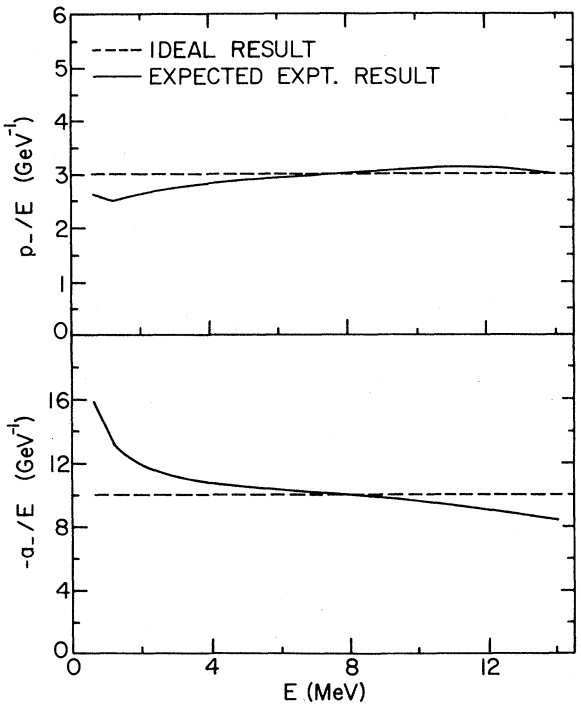

FIG. 9. Calculated effect of the convolution with the beta detector response function on the ^{8}Li β-α angular correlation coefficients. The coefficients are divided by the beta energy E to show the effect on the slopes of a_- and p_- as a function of E. Note that the average slope is essentially unaffected.

E. Systematic experimental errors

A summary of the estimated uncertainties in the β-α angular correlation data associated with the various issues raised in this section is shown in Table I. The term "other β detector effects" refers to the corrections that were introduced to remove β detector resolution (energy response) effects and asymmetries between the β counters. The 2% uncertainty quoted for this class of effects allows for a 20% error in the calculation of these corrections, although reasonable variations in the width of the response functions only induced changes of about 5%.

TABLE I. Estimates of systematic errors in the β-α angular correlation measurement.

Source	Uncertainty in $a_{\pm}/E$, $p_{\pm}/E$
β-energy calibration	1%
Other β detector effects	2%
Geometric effects	1%
Quadratic sum	2.4%

F. Analysis of β-ν-α correlations

The coincident events were also analyzed for the β-ν-α correlation discussed in Sec. II. Arrays were constructed of $\sum E_\alpha$ vs ΔE_α with windows set on the TAC coincidence peak and beta particle energy. The beta-energy window was about 0.5 MeV wide at ~6.5 MeV. Four spectra $F(0)_1$, $F(90)_1$, $F(90)_2$, and $F(180)_2$ were used, where 0, 90, and 180 refer to $\theta_{\beta\alpha}$, and 1 and 2 correspond to *alpha* detector pairs 1+3 and 2+4, respectively.

For each $\sum E_\alpha$, the centroid in ΔE_α was calculated for each spectrum, giving the four sets of centroids $C(0)_1$, $C(90)_1$, $C(90)_2$, and $C(180)_2$. These were then combined in the following manner:

$$\langle \Delta E_\alpha \rangle_1 = C(0)_1 - C(90)_1 - 5 \text{ keV}, \quad (9a)$$

$$\langle \Delta E_\alpha \rangle_2 = C(180)_2 - C(90)_2 + 20 \text{ keV}, \quad (9b)$$

where the 5 and 20 keV corrections account for β-energy loss in the silicon detectors, and the $C(90)$ terms eliminate effects due to the distribution of source activity within the target foil.

These quantities are quite insensitive to the large effects induced by the finite source foil thickness on the individual $F(\theta)_i$. The first order corrections will come from the α-energy dependence of the stopping power in the source foil. This effect is calculated to be <2 keV in this region of α energy, and hence is a small effect on $\langle \Delta E_\alpha \rangle$, which is typically 150 keV.

VI. RESULTS AND DISCUSSION

A. β-ν-α correlations

The experimental values of $\langle \Delta E_\alpha \rangle$ [defined in Eq. (9)] for $E \cong 6.5$ MeV are plotted versus E_x in Fig. 10. The results indicate that the Gamow-Teller nature of the decay persists throughout the energy region $2 < E_x < 8$ MeV. The presence of any Fermi decay strength would imply isospin mixing with the $T=1$, $T_z=0$ analog of the ground states of ^{8}Li and ^{8}B. The isovector contributions from the tails of the 16.6 and 16.9 MeV states interfere destructively in this energy region according to an R-matrix analysis.[11] In addition, shell model wave functions[12] predict the 2.9-MeV state to be predominantly ^1D while the $T=1$ state is mostly ^3P in a basis with four particles in the p shell. The mismatch in the spin parts of these wave functions would probably lead to a very small isospin violating Coulomb matrix element. Thus, the apparent absence of Fermi decay strength is not a surprising result.

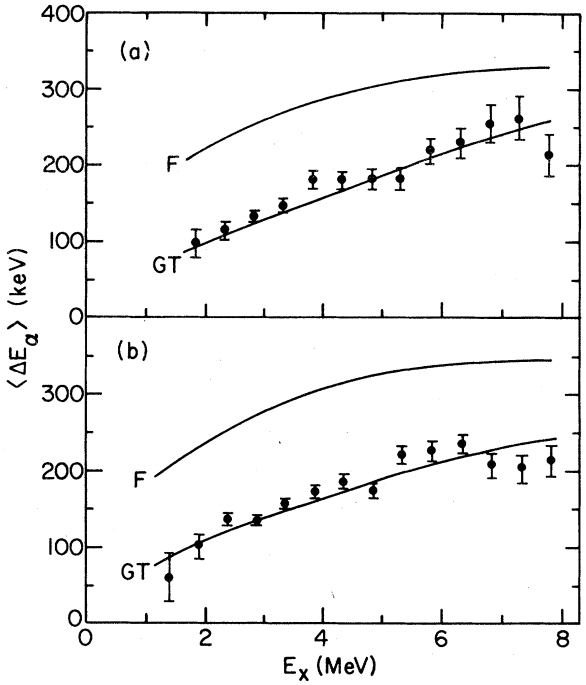

FIG. 10. Experimental results for the β-ν-α correlation as a function of the final-state excitation energy in ^{8}Be: (a) ^{8}Li decay, (b) ^{8}B decay. The quantity $\langle \Delta E_\alpha \rangle$ is defined in Eq. (9) and the curves F (Fermi) and GT (Gamow-Teller) are calculated from Eq. (6) with $\rho = +1$ and $\rho = -1$, respectively.

B. $\beta^{\pm}$-α angular correlations: cos(θ) term

Since the results of the β-ν-α correlation analysis indicate that the decays are pure Gamow-Teller, the correct expressions for $a_{\mp}$ are given by Eq. (2). The experimental data for $a_{\mp}/E$ (the slopes of $a_{\mp}$), analyzed without regard for final-state energy, are shown in Fig. 11. The agreement between the experimental data and theoretical curves is quite good, and the anomalous behavior ($a_{\mp}/E$ both ~10% too low) reported by a previous experiment[8] is not present. It was found, however, that the results for $a_{\mp}/E$ are quite sensitive (~10% variations were observed) to several experimental effects, notably source foil quality (torn or otherwise damaged) and alpha signal discriminator thresholds. The coefficients

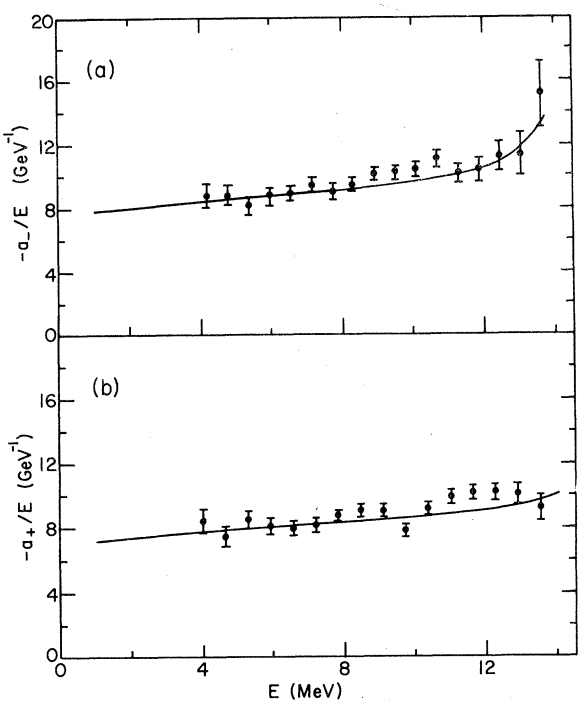

FIG. 11. The negatives of the slopes of the $a_\mp$ coefficients as a function of beta energy when the data are analyzed independent of final-state energy. The solid curves are calculated from Eq. (2), appropriately averaged over the final-state distribution, with $p_-/E=3$ GeV GeV^{-1} and $p_+/E=-4$ GeV^{-1}.

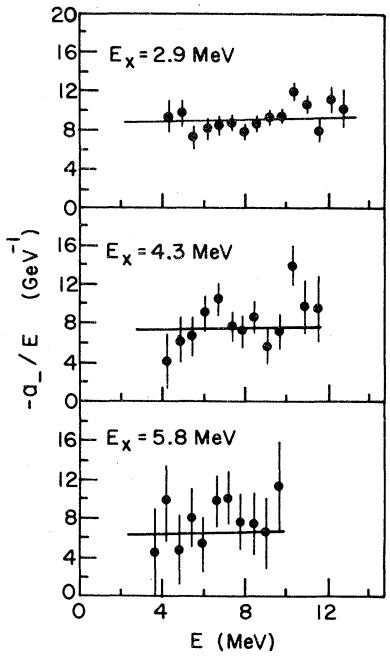

FIG. 12. The negatives of the slopes of the a_- coefficient as functions of beta energy at various final-state energies. The solid curves are calculated from Eq. (2) using $p_-/E=3$ GeV^{-1}.

$p_\mp/E$ were found to be rather insensitive to these effects. In addition, it should be noted that the beta-energy calibration was handled in a very different way from previous experiments.

Plots of the experimental data for $a_\mp/E$ at several individual E_x values are shown in Figs. 12 and 13. Again the solid curves are calculated from Eq. (2) and are in good agreement with the data. At each E_x, the weighted mean of $a_\mp/E$ was calculated for $E_0/3<E<(E_0-0.5$ MeV). These average slopes are shown in Fig. 14, again with the theoretical predictions shown as solid curves. The fact that the excitation energy dependences of a_+/E and a_-/E are well represented by the experimental data supports the conclusion that the same procedures used to extract the coefficients p_+/E and p_-/E do yield meaningful results.

In anticipation of the calculation of δ^-, the difference $a_-/E-a_+/E$ of the average slopes is plotted in Fig. 15 as a function of the excitation energy in ^{8}Be. The good agreement with the expected solid curve indicates the lack of some serious systematic errors which might contribute to the quantity δ^-.

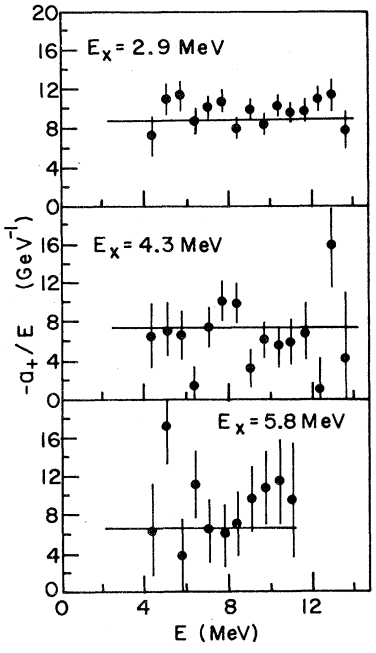

FIG. 13. Same as Fig. 12 for the a_+ coefficient. The value $p_+/E=-4$ GeV^{-1} was used in Eq. (2) to calculate the solid curves.

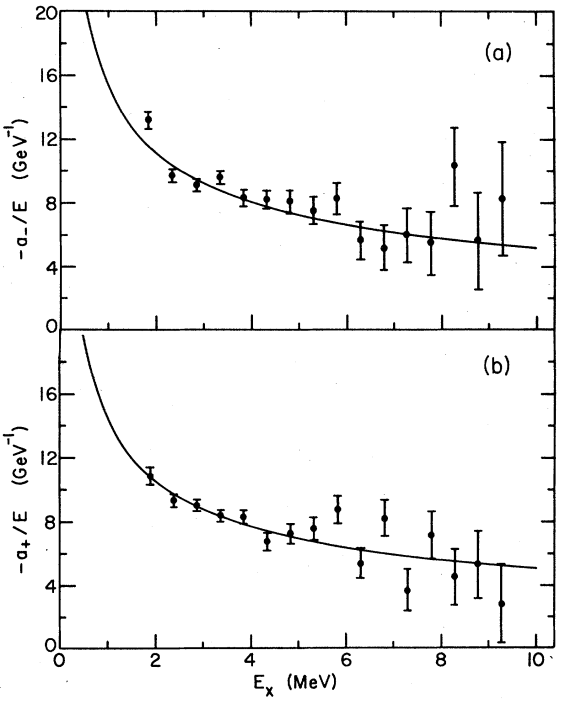

FIG. 14. The negatives of the average slopes of the $a_\mp$ coefficients as functions of E_x, the final-state energy relative to the ^{8}Be ground state. The solid curves are calculated from Eq. (2).

C. $\beta_\pm$-α angular correlation: $\cos^2(\theta)$ term

The results of the analyses of p_-/E and p_+/E, integrated over final-state energy, are shown in Fig. 16. Figure 17 shows the result for δ^- (without regard for final-state energy) from this work, and the prediction of Bowles *et al.*[6] who invoked CVC to calculate δ^- from the properties of the analog γ decay. Their calculation yields $\delta^-_{EM} = 8.45 \pm 1.1$, whereas our result [assuming $\delta^-(m_n/E)$ is independent of E] is $\delta^-_{\beta-\alpha}(m_n/E) = 6.5 \pm 0.2$, in good agreement with the value reported by Tribble *et al.*[8] $\delta^-_{\beta\alpha}(m_n/E) = 7.0 \pm 0.5$.

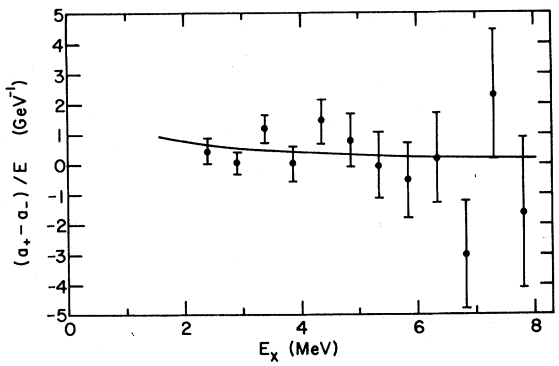

FIG. 15. The difference of the average slopes of the a coefficients as a function of final-state energy. The solid curve is from Eq. (2).

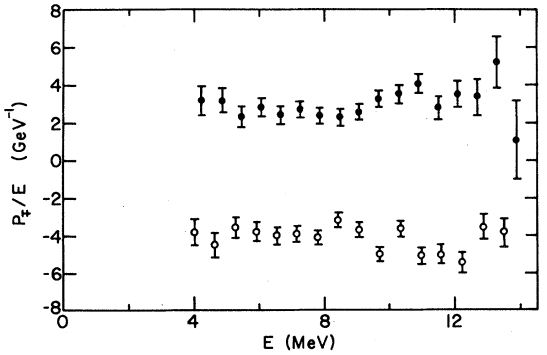

FIG. 16. The slopes of the $p_\mp$ coefficients vs beta energy when the data are analyzed without regard for final-state energy. The solid dots are p_-/E (^{8}Li decay) and the open circles are p_+/E (^{8}B decay).

One expects small contributions to $\delta^-_{\beta\alpha}$ from electromagnetic effects. The mismatch in E_0 between β^+ and β^- decays leads to a residual contribution from the j_2 form factor in δ^- which has the effect of increasing $\delta^-_{\beta\alpha}(m_n/E)$ by ~0.07. There are also induced Coulomb effects, which are calculated by Holstein[13] to contribute −0.23 to $\delta^-_{\beta\alpha}(m_n/E)$. In addition, there are effects associated with the fact that the ground states of ^{8}Li and ^{8}Be are not exact isotopic analogs (due to Coulomb effects), which may affect the value $\delta^-_{\beta\alpha}(m_n/E)$ by 5–10% [e.g., $c^2(^8\mathrm{B}) \cong 0.9\,c^2(^8\mathrm{Li})$]. Simple radial overlaps of p-shell nuclear wave functions (chosen to match the observed separation energies and including Coulomb effects) reproduce the ft asymmetry quite well. Similar calculations of the radial matrix elements of r^2 show that, at least in the impulse approximation, the Coulomb-induced effects on the second-forbidden form factors are also small. It would be difficult to understand a nuclear Coulomb contribution to $d^{\mathrm{eff}}_{\mathrm{II}}/Ac$ of more than 0.5.

Combining $\delta_{\beta\alpha}$, δ_{EM}, and the above corrections, yields the value $d^{\mathrm{eff}}_{\mathrm{II}}/Ac = 1.8 \pm 1.1$, where the uncertainty reflects only experimental sources of error. This result depends crucially on the use of CVC to include the weak analog of the quadrupole term in the electromagnetic current, since without it (including only weak magnetism) one would obtain $\delta^-_{\mathrm{EM}}(M_n/E) = 10.9 \pm 1.4$,[6] a serious discrepancy with the β-α angular correlation measurements. In the analysis above, the $E2/M1$ mixing ratio was assumed linear in gamma-ray energy, and the uncertainty in $d^{\mathrm{eff}}_{\mathrm{II}}/Ac$ does not include the uncertainty associated with this assumption.

As can be seen in Fig. 17, the result for $\delta^-(m_n/E)$ seems to show a small positive slope, and,

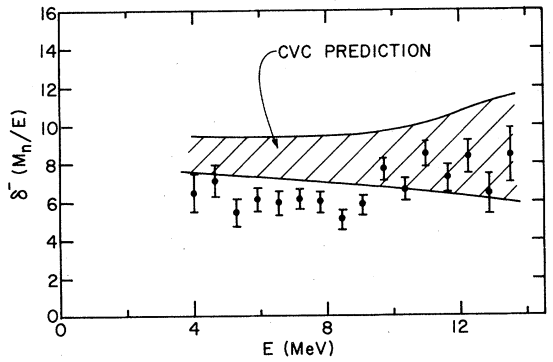

FIG. 17. The slope of δ^- as a function of beta energy for the data analyzed independent of final-state energy. The indicated band is the CVC prediction calculated by Bowles *et al.*[6]

in fact, a least squares fit does yield a positive slope of (0.22 ± 0.07) MeV^{-1}. This is somewhat difficult to interpret, especially since the corrections applied to account for the β detector resolution involve slopes of this magnitude, and the accuracy of those calculations is not well known. For this reason, it was concluded that analyzing the slopes to draw conclusions about second-forbidden terms would not be particularly useful.

In analogy to the treatment of $a_\mp/E$, the weighted means for the slopes (again for $E_0/3 < E < E_0 - 0.5$ MeV) $p_\mp/E$ were calculated at each excitation energy, and the difference formed to give δ^-/E. The results for $\delta^-(m_n/E)$ are shown in Fig. 18 as a function of excitation energy in ^{8}Be. Also shown in Fig. 18 is the CVC prediction calculated from the data of Bowles *et al.*[6] with $\delta_1(E_x)$ assumed to be linear with gamma-ray energy. The agreement is quite good except for a small discrepancy at lower excitation energies.

However, it does appear that both measurements (independent of excitation energy) of the β-α angular correlation deviate from the CVC prediction due to a small discrepancy at low excitation energies ($E_x \lesssim 3.5$ MeV). If this effect were to be attributed to a second-class induced tensor form factor d_{II}, the ft-value asymmetry would show a very large end-point-energy dependence which would contradict the results of the experiment performed by Wilkinson and Alburger.[9] Therefore, if the origin is a second-class axial vector current, it must be arising from the second-forbidden form factors j_2 and j_3.

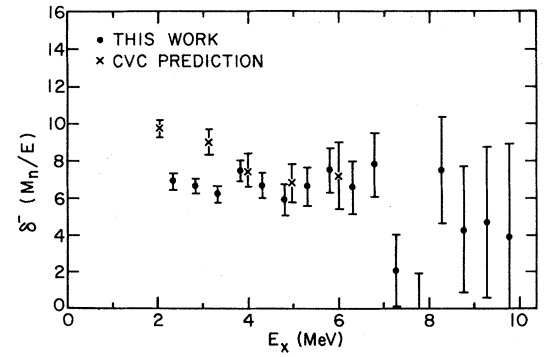

FIG. 18. Average slope of δ^- as a function of final-state excitation energy. The CVC prediction is from the data of Bowles *et al.*[6]

Another possibility is that the assumed E_x dependence of the $E2/M1$ mixing ratio is incorrect. In particular, if $\delta_1(E_x)$ were more positive at lower excitation energies and changed sign at higher E_x to keep the average experimental value $\delta_1 = 0.2$, the agreement with the β-α correlation data would be substantially improved. Although it is very difficult experiment, a more detailed measurement of $\delta_1(E_x)$ would be extremely helpful in clarifying the interpretation of these results. In fact, although the analog gamma width is a well corroborated result,[6,14,15] there is only one measurement of the $E2/M1$ mixing ratio, and further experimental work substantiating that result would be useful.

VII. SUMMARY

A small final-state energy-dependent deviation from the CVC prediction is observed in the $A = 8$ system. This discrepancy (~15% of the weak magnetism term) is sensitive to the assumption of the final-state energy dependence of δ_1, the isovector $E2/M1$ mixing ratio of the analog gamma decay. However, since a large anomalous effect is introduced if one ignores the vector second-forbidden terms predicted by CVC from δ_1, these experiments represent approximate confirmation of CVC at the second-forbidden level.

In contrast to the situation of a few years ago, there are now several experiments in other nuclear systems which are consistent with the absence of SCC and the validity of CVC (weak magnetism). Recent results in the $A = 12$ and $A = 20$ systems yield the values $d_{II}/Ac = 0.0 \pm 0.5$ (Ref. 16) and $d_{II}/Ac = 0.3 \pm 0.8$,[17] respectively, and it appears that the earlier measurements of beta asymmetries in $A = 12$ (Ref. 18) and $A = 19$ (Ref. 19) which reported large SCC were erroneous. Therefore, the relatively small discrepancy observed in the mass 8 experiments cannot be interpreted as conclusive evidence for the presence of SCC or a breakdown of CVC.

The rather unique sensitivity of the $A = 8$ experiments to the second-forbidden vector current effects makes them useful for further experimental

studies of CVC. In this regard, further experimental work on the analog gamma-decay properties is clearly desirable.

ACKNOWLEDGMENTS

We would like to acknowledge several enlightening conversations with Dr. B. Holstein and Dr. T. Bowles. The assistance of A. Davis during data acquisition is gratefully acknowledged. We would also like to thank the technical staff and Dynamitron operations staff at the Argonne Physics Division for their support. This work was performed under the auspices of the U. S. Department of Energy.

[1]B. R. Holstein, Rev. Mod. Phys. 46, 789 (1974).
[2]R. P. Feynman and M. Gell-Mann, Phys. Rev. 109, 193 (1958).
[3]S. Weinberg, Phys. Rev. 112, 1375 (1958).
[4]P. Langacker, Phys. Rev. D 15, 2386 (1977).
[5]K. Kubodera, J. Delorme, and M. Rho, Phys. Rev. Lett. 38, 321 (1977).
[6]T. J. Bowles, Ph.D. thesis, Princeton University (unpublished).
[7]T. J. Bowles and G. T. Garvey, Phys. Rev. C 18, 1447 (1978).
[8]R. E. Tribble and G. T. Garvey, Phys. Rev. C 12, 967 (1975).
[9]D. H. Wilkinson and D. E. Alburger, Phys. Rev. Lett. 26, 1127 (1971); D. H. Wilkinson and D. E. Alburger, private communication.
[10]J. F. Ziegler and W. K. Chu, At. Data Nucl. Data Tables 13, 463 (1974).
[11]F. C. Barker, Aust. J. Phys. 22, 293 (1969).
[12]F. C. Barker, Nucl. Phys. 83, 418 (1966).
[13]B. R. Holstein, Phys. Rev. C 19, 1467 (1979).
[14]P. Paul, M. Suffert, and Ph. Gorodetzky, Phys. Lett. 71B, 71 (1977).
[15]P. Long and D. A. Bromley, in *Proceedings of the International Conference on Nuclear Structure, Tokyo, 1977*, edited by T. Marumori (Physical Society of Japan, Tokyo, 1978).
[16]H. Brändle, G. Miklos, L. Ph. Roesch, V. L. Telegdi, P. Truttman, A. Zehnder, L. Grenacs, P. Lebrun, and J. Lehmann, Phys. Rev. Lett. 41, 299 (1978).
[17]N. Dupuis-Rolin, J. P. Deutsch, D. Favart, and R. R. Prieels, Phys. Lett. 79B, 359 (1978).
[18]K. Sugimoto, I. Tanihata, and J. Göring, Phys. Rev. Lett. 34, 1533 (1975).
[19]F. P. Calaprice, S. J. Freedman, W. C. Mead, and H. C. Vantine, Phys. Rev. Lett. 35, 1566 (1975).